Enhanced thermoelectric properties of Mg$_2$Si by addition of TiO$_2$ nanoparticles

D. Cederkrantz,[1,a)] N. Farahi,[1] K. A. Borup,[2] B. B. Iversen,[2] M. Nygren,[3] and A. E. C. Palmqvist[1]

[1]*Department of Chemical and Biological Engineering, Chalmers University of Technology, SE-41296 Göteborg, Sweden*
[2]*Center for Materials Crystallography, Department of Chemistry, Aarhus University, DK-8000 Aarhus C, Denmark*
[3]*Department of Inorganic Chemistry, Arrhenius Laboratory, Stockholm University, SE-10691 Stockholm, Sweden*

The effects on the thermoelectric properties of Mg$_2$Si when adding TiO$_2$ nanoparticles have been evaluated experimentally. A batch of Mg$_2$Si was prepared through direct solid state reaction and divided into portions which were mechanically mixed with different amounts of TiO$_2$ nanoparticles ranging from 0.5 to 3 vol% and subsequently sintered to disks. All materials showed n-type conduction and the absolute value of the Seebeck coefficient was reduced with increasing amount of TiO$_2$ added, while the electrical resistivity was greatly reduced. The thermal conductivity was surprisingly little affected by the addition of the nanoparticles. An optimum value of the thermoelectric figure-of-merit ZT = TS$^2\sigma$/k was found for the addition of 1 vol% TiO$_2$, showing almost three times higher ZT value than that of the pure Mg$_2$Si. Larger TiO$_2$ additions resulted in lower ZT values and with 3 vol% added TiO$_2$ the ZT was comparable to the pure Mg$_2$Si. The sintering process resulted in reduction or chemical reaction of all TiO$_2$ to TiSi$_2$ and possibly elemental titanium as well as reduced TiO$_x$. The increased electrical conductivity and the decreased Seebeck coefficient were found due to an increased charge carrier concentration, likely caused by the included compounds or titanium-doping of the Mg$_2$Si matrix. The low observed effect on the thermal conductivity of the composites may be explained by the relatively higher thermal conductivity of the included compounds, counter-balancing the expected increased grain boundary scattering. Alternatively, the introduction of compounds does not significantly increase the concentration of scattering grain boundaries. © *2012 American Institute of Physics*. [doi:10.1063/1.3675512]

INTRODUCTION

Over the last two decades the demand for more efficient use of energy has triggered a renewed interest in finding new and improved thermoelectric materials. The interest in these semiconductors, in the context of energy applications, is due to the possibility of using thermoelectrics for direct conversion of thermal energy into electricity. Utilizing this phenomenon, thermoelectric generators (TEGs) for waste heat recovery are constructed without any moving parts and can therefore be made compact and with very low maintenance requirements. With such generators the fuel economy of any type of small to medium size energy conversion process that generates heat could be improved.[1] This makes the technique attractive, e.g., the automotive industry in its efforts to minimize CO$_2$ emissions and reduce fuel consumption.[2] In this kind of application a TEG can be beneficial even with a relatively low conversion efficiency of 5%–10%.[3]

The functional unit of a TEG is a set of thermoelectric materials exhibiting n- and p-type conductivity, respectively, connected electrically in series and thermally in parallel. The performance of these thermoelectric materials is characterized by their Seebeck coefficient (S), electrical conductivity (σ), and thermal conductivity (κ). These properties can be combined in the dimensionless figure-of-merit ZT = $TS^2\sigma/\kappa$, where T is the absolute temperature of operation. A good thermoelectric material has a high ZT value, but achieving high ZT values is no easy task since the thermoelectric properties are derived from the same electronic energy function. In the mid-1990s Slack[4] presented the concept of the phonon glass electron crystal (PGEC), in which it was proposed that certain host-guest crystal structures should be able to conduct electricity like a crystal and heat like a glass, thus becoming an ideal thermoelectric material. This new hypothesis and the increased interest in energy efficiency applications have resulted in a number of novel and complex thermoelectric bulk materials, e.g., skutterudites and clathrates, with ZT values above unity.[5] To reach even higher ZT values delicate materials engineering is required, such as reducing the dimensions of the material into the nanosize range as first suggested and later experimentally demonstrated by Dresselhaus and co-workers.[6–9] Applying nanotechnology following these initial theories has since resulted in great improvements of the thermoelectric properties of such materials in the form of nanocomposites,[10–12] superlattices,[13,14] and nanostructures.[15,16]

During the last decade, theoretical[17,18] and experimental[19–23] studies have been carried out to utilize the benefits of nanostructuring in bulk materials by, e.g.,

a)Author to whom correspondence should be addressed. Electronic mail: daniel.cederkrantz@chalmers.se.

embedding insulating or conducting nanoparticles into bulk TE materials. These nanoparticles are often referred to as nano-inclusions and they can improve the thermoelectric properties of a material in several ways. Firstly, the nanoparticles will introduce new interfaces which may scatter phonons and electrons differently. If the inclusions are properly selected in concentration and size they will reduce the thermal conductivity of a material more than the electrical conductivity since, at least at low temperatures, the mean free path of a phonon is longer than that of an electron or hole, thus ZT can be improved.[16] Secondly the Seebeck coefficient can be improved by a process known as energy filtering of the electrons. This is achieved by bending the electron bands at the interfaces between the inclusions and the bulk matrix allowing electrons with high energy to pass, while scattering the slow electrons. The selective scattering increases the value of the Seebeck coefficient and requires suitable types of material to be used in the nano-inclusions to achieve a beneficial band bending.[24,25] The actual potential for improving ZT with electron filtering has recently been debated,[18] but it has also been shown that it is possible to simultaneously improve the power factor ($S^2\sigma$) and reduce the thermal conductivity with the use of nanoparticles.[26] A third possible effect of introducing nano-inclusions is that they may tune the charge carrier concentration by acting either as charge donors or charge acceptors to the matrix.

Magnesium silicide (Mg_2Si) is a semiconductor with rather poor thermoelectric properties, but great potential for improvement, e.g. by forming a solid solution with Mg_2Sn doped with Sb (Refs. 27 and 28) or by doping pure Mg_2Si with P or Bi.[29,30] The elements in Mg_2Si are abundant in nature and environmentally friendly, which makes it attractive from a sustainability perspective. Recently it has been shown that small amounts of TiO_2 nanoparticles in skutterudites are effective for increasing ZT by slightly reducing thermal conductivity as well as improving the Seebeck coefficient to some extent.[31] In this paper the effects on the thermoelectric properties, as well as the charge carrier concentration and mobility, of introducing inclusions of TiO_2 nanoparticles in Mg_2Si have been evaluated.

Experimental methods

Synthesis of thermoelectric materials

Magnesium silicide materials containing different concentrations of nanoparticulate TiO_2 in the range of 0–3 vol% were prepared as follows. Pure elements of Mg and Si (99.95%, Sigma-Aldrich) were mixed in a glovebox (high-purity Ar atmosphere) in a 2% excess of Mg compared to stoichiometry to compensate for evaporation of Mg during the reaction. The mixed powders were ground 2×20 min to a homogeneous mixture with a Mixer Miller (MM400 from Retsch). The mixture was annealed in a tube furnace (Entech, with a Eurotherm controller) at 600 °C for 24 h under argon atmosphere with 5% hydrogen to reduce surface oxides. The thus prepared magnesium silicide powder was then sieved through an 80 μm mesh before further processing.

Desired amounts of TiO_2 (anatase, 99.7%, 15 nm, Alfa Aesar) were subsequently mixed with batches of the prepared Mg_2Si using the Mixer Miller for 2×15 min to prepare homogenous mixtures without visible agglomerates. The obtained Mg_2Si/TiO_2 powders were compacted by spark plasma sintering (SPS) at 725 °C for 5 min under a pressure of 75 MPa yielding disks with a diameter of 12 mm, a thickness of 6–7 mm, and a density of >95% of the theoretical density. The disks were used for measurements of thermoelectric properties as described below.

Structural characterization

X-ray diffraction was performed on the powders of the prepared thermoelectric materials using a Bruker XRD D8 advance utilizing monochromatic Cu $K_{\alpha 1}$ radiation. Data were collected on powders before sintering covering a 2θ range of 20°–60° with a step size of 0.0289° and a step time of 1 s. For selected sintered disks and the pure Mg_2Si powder the experiment was repeated with smaller step size, 0.00263°, and longer step time, 3 s, to enhance the resolution of the diffractogram. During the measurements the samples were rotated with a speed of 60 and 20 rpm, respectively.

SEM and EDX characterization were performed on sintered disks with a Leo Ultra 55 FEG to confirm sample homogeneity and nominal chemical composition.

Measurement of thermoelectric properties

Thermal conductivity (κ) was measured as described previously[32] using a Hot Disk TPS 2500 S instrument based on the transient plane source (TPS) technique.[33] Each disk of sintered thermoelectric material was cut into two disks with a diamond saw to enable double-sided measurements to be carried out and thus to maintain uniform heat dissipation from both sides of the sensor sandwiched between the two disks during the measurements. Room temperature measurements were performed in an ambient atmosphere with a Kapton-insulated Ni TPS-element as the sensor. Measurements for higher temperatures up to 700 °C were carried out under helium atmosphere using mica-insulated Ni elements.

The electrical resistivity ($1/\sigma$) and Seebeck coefficient (S) were measured simultaneously under low pressure He atmosphere from room temperature to 700 °C using a ZEM-3 instrument from Ulvac-Riko. Measurements were performed on bar-shaped specimens with a width of 2.5–3.5 mm and a length of 8–10 mm cut from the sintered disks of thermoelectric materials. To determine the thermopower a static DC method is used to measure a potential difference (ΔV) induced by a temperature difference (ΔT) over a well-defined length of the specimen bar, which gives $S = \Delta V/\Delta T$. The electrical resistivity is calculated using the relation $1/\sigma = R \cdot A/d$, where R is the resistance measured by the 4-point probe method (R = V/I), A is the cross section area of the specimen bar, and d is the distance between the probes used to measure the voltage difference.

Measurements of charge carrier concentration and charge carrier mobility were carried out using a Physical Property Measurement System (PPMS) by Quantum Design equipped with a 9 T magnet. The geometry of the analyzed specimens was thin (500 μm) rectangular (10×2 mm) slices cut from the bars used for Seebeck and electrical resistivity

measurements. Measurements were carried out at 300 and 395 K and each measurement was carried out in ten steps, increasing the magnetic field from 0 to 9 T before flipping the sample 180° and then reducing the magnetic field from 9 to 0 T in ten more steps.

RESULTS AND DISCUSSION

Structural characterization of prepared materials

The normalized powder X-ray diffractogram of the prepared Mg_2Si powder shown in Fig. 1(a) (diffractogram 1) is in good agreement with literature data.[34,35] Normalization was performed by giving the main diffraction peak an intensity of 1000. Trace amounts of silicon and MgO could be identified in the powder as a result of incomplete synthesis. After spark plasma sintering (diffractogram 2) the intensity of the Si and MgO peaks in the diffractogram increased, suggesting a small decomposition of Mg_2Si during the sintering process. For the samples to which TiO_2 was added no traces of TiO_2 could be detected in any of the diffractograms after sintering. Instead the relative intensities of the MgO peaks increased compared to the Si peaks as illustrated for the sample to which 3 vol% TiO_2 was added (diffractogram 3). In addition, in the magnified diffractograms shown in Fig. 1(b),
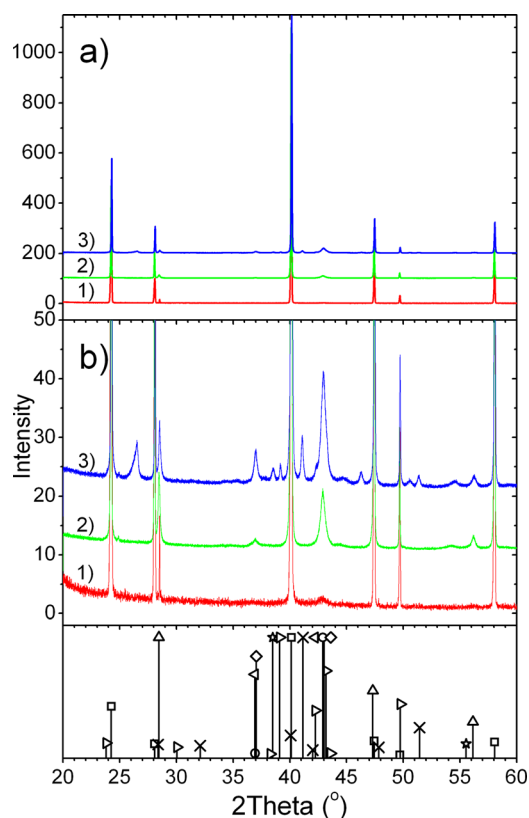
FIG. 1. (Color online) Normalized powder X-ray diffractograms (a) and magnification of the background of the diffractograms (b) of 1) as synthesized Mg_2Si powder, 2) sintered Mg_2Si reference without TiO_2 nanoparticles, and 3) sintered Mg_2Si with 3 vol% TiO_2 nanoparticles added, along with the relative intensities of the identified phase. Legend: Mg_2Si (□) PDF #04-001-3251, MgO (○) PDF #00-045-0946, Si (Δ) PDF #04-001-7247, Ti (☆) PDF #00-044-1288, $TiO_{0.71}$ (◇) PDF #04-005-6498, $TiO_{0.84}$ (◁) PDF #04-006-1902, $TiSi_2$ (▷) PDF #04-007-1144, and $TiSi_2$ (×) PDF #04-002-1352.

two $TiSi_2$ phases (PDF #04-007-1144 and #04-002-1352, the latter being a metastable phase formed prior to the stable orthorhombic phase[36]) were observed and possibly minute amounts of a high temperature Ti phase (PDF #00-044-1288). These observations are consistent with a scenario in which the TiO_2 reacts with Mg_2Si or elemental Si present in the sample to form MgO, $TiSi_2$ and possibly Ti. Another possibility is formation of reduced TiO_x, which cannot be completely ruled out since both $TiO_{0.71}$ and $TiO_{0.84}$ phases (PDF #04-005-6498 and #04-006-1902) show significant overlap with the MgO phase, and can therefore not be separated within the 2Θ range. The relative increase in the MgO peaks compared to the Si peaks could thus be an indication of the formation of reduced TiO_x. It is also likely that some of the titanium has entered the Mg_2Si structure as a dopant due to the strong direct current passing through the sample during the SPS procedure. If Ti enters the structure as a dopant it would donate electrons to the structure and thus increase the charge carrier concentration.

Using the Scherrer[37] equation it is concluded that the Mg_2Si grains are larger than 100 nm, the large grain size making the Scherrer equation imprecise for more accurate size determination. Both $TiSi_2$ phases are calculated to be in the diameter range of 30–40 nm and the possible titanium phase grains has a slightly larger diameter of approximately 60 nm. Due to the large overlap between MgO and the TiO_x phases meaningful calculations were not possible to perform with the available XRD data. However, these calculations confirm that nanoparticles are present in the prepared materials.

In the diffractogram of the sample to which 3 vol% TiO_2 was added a graphite peak is also present due to residue from the SPS process on the sample surface. Elemental analysis based on EDX measurements ($20 \times 20\,\mu m^2$ area) on the disks confirmed that the nominal amount of titanium in the materials was in agreement with the amounts used in the synthesis and low resolution SEM microscopy showed that all disks were homogenously compacted and free from large cracks.

Thermopower of prepared materials

The temperature dependence of the Seebeck coefficient of all prepared Mg_2Si-based materials is shown in Fig. 2. All materials show n-type conduction as seen by the negative values of the measured Seebeck coefficients. A clear trend is revealed in the presented graph, showing that the room temperature thermopower of the materials decreases with increased titanium content. This indicates a shift toward a more conducting material with increased concentration of titanium present in the material. The trend seen in the series of materials is consistent over the entire temperature range for all materials prepared with TiO_2, while the reference sample has a sharper decline in absolute Seebeck values up to 350 °C, above which it followed a similar trend as the material with 1.5 vol% TiO_2 added. The maximum absolute Seebeck values occurred around 200 °C for the materials with the lowest amount of added TiO_2 nanoparticles but gradually shift to lower temperatures for materials with more
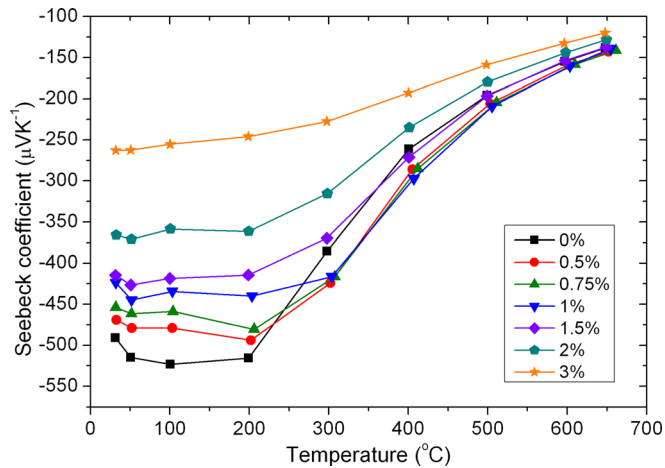
FIG. 2. (Color online) Seebeck coefficient of Mg_2Si with the addition of 0–3 vol% TiO_2 nanoparticles. The measurement error with the ZEM-3 is typically $\pm 10\%$.

added TiO_2 and for the material with 3 vol% TiO_2 added the maximum appears to occur below the measured temperature range indicating a more narrow bandgap in accordance with the equation $E_g \approx 2S_{max}T_{max}$.[38] The observed effects of the TiO_2 addition on the thermopower are consistent with the reduction and reaction of TiO_2 during sintering, since the SPS procedure likely allows titanium to enter the crystal structure of Mg_2Si. If titanium is incorporated in the Mg_2Si matrix it will act as a dopant and as such donate charge carriers to the bulk material and reduce the absolute Seebeck coefficient as well as the electrical resistivity.

Electrical transport properties of the prepared materials

The electrical resistivity of Mg_2Si was greatly affected by the introduction of TiO_2 nanoparticles as seen in Fig. 3. The room temperature resistivity of the Mg_2Si reference sample free from TiO_2 was almost 460 mΩ cm in comparison to 53 mΩ cm of the material prepared with 3 vol% TiO_2. Even the smallest addition of TiO_2 (0.5 vol%) resulted in
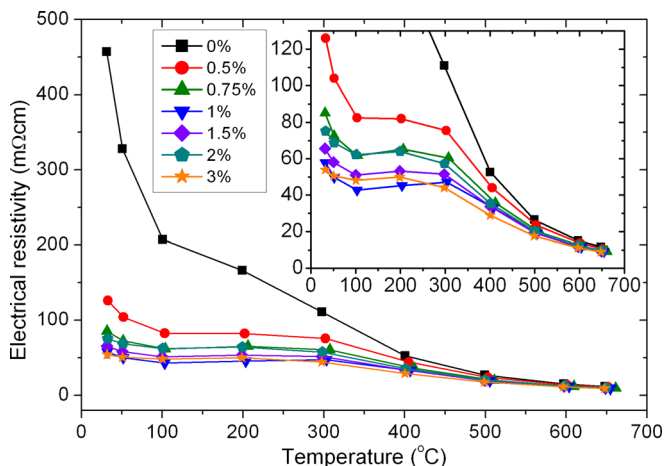
FIG. 3. (Color online) Electrical resistivity of Mg_2Si with the addition of 0–3 vol% TiO_2 nanoparticles with an inset showing the details at lower resistivity.

significant reduction of room temperature resistivity to 126 mΩ cm. The room temperature resistivity of the other materials falls between these two latter values, whereas the 1 vol% sample shows the lowest overall resistivity over the entire remaining temperature range. The resistivity of all materials prepared is semiconductor-like and thus decreases with increasing temperature and exhibiting a shoulder around 200–300 °C. At the maximum measured temperature all materials have similar resistivity around 10 mΩcm.

Again it is reasonable to propose that the reduction and reaction of the introduced TiO_2 during sintering results in donation of electrons to the bulk material, which thus reduce its resistivity. Otherwise the electrical resistivity would presumably have increased instead due to increased grain boundary scattering caused by the nano-inclusions.

Charge carrier concentration and mobility of prepared materials

The charge carrier concentration and mobility of the Mg_2Si material with no added TiO_2 are compared to the materials prepared with 1 and 3 vol% TiO_2 nanoparticles in Table I. The data clearly confirm the hypothesis that an increase in titanium content in the material increases the charge carrier concentration. As expected the concentration of charge carriers increases with temperature for all three materials. The presence of titanium in the samples with TiO_2 addition and the correlation between the amount of added TiO_2 and the charge carrier concentration clearly suggest that the charge carrier concentration in Mg_2Si is tunable through the addition and subsequent reduction and chemical reaction of TiO_2 nanoparticles. Most likely titanium atoms are incorporated into the Mg_2Si matrix during the sintering process. It should be noted that the pure Mg_2Si material shows a charge carrier concentration a factor 10 higher than what has been reported for an undoped single crystal of Mg_2Si, while the charge carrier concentration of the samples with added TiO_2 is in the same range as reported for single crystals of Mg_2Si doped with Al or Ag.[39] It is also possible that the observed $TiSi_2$ phases could affect the charge carrier concentration through donation over the junction with the Mg_2Si grain boundaries, but the effect of such a process will be negligible compared to the effect achieved through titanium doping into the Mg_2Si lattice, as estimated from simple calculations.

The mobility of the charge carriers of the three materials presented in Table I is in the same range for all three materials at 27 °C, around 150 cm^2/Vs. However, at 122 °C the pure Mg_2Si material showed more than doubled charge carrier mobility compared to the mobility at 27 °C. For the material with 1 vol% TiO_2 added the increase is much smaller, only around 17%, whereas the material with 3 vol% TiO_2 added exhibits a decrease in charge carrier mobility of 30%, presumably due to an increased frequency of collisions between the charge carriers as they become more numerous.

Thermal conductivity of prepared materials

The thermal conductivity of all prepared materials is shown as a function of temperature in Fig. 4. The expected

TABLE I. Charge carrier concentration and mobility of selected Mg_2Si-based materials at 27 and 122 °C.

Material	Temperature (°C)	Charge carrier conc. (cm^{-3})	Charge carrier mobility (cm^2/Vs)
Pure Mg_2Si	27	2.9×10^{17}	143
	122	3.5×10^{17}	284
Mg_2Si with	27	1.3×10^{18}	164
1 vol% TiO_2	122	1.6×10^{18}	193
Mg_2Si with	27	1.7×10^{18}	151
3 vol% TiO_2	122	2.6×10^{18}	103

result of adding and increasing the concentration of nano-inclusions was to reduce the thermal conductivity of the material, but as seen in the graph all materials show quite similar values. All prepared materials exhibit a room temperature thermal conductivity in the range of 9–10 W m^{-1} K^{-1} which is reduced to a minimum of around 4.5 W m^{-1} K^{-1} at temperatures slightly above 400 °C followed by an increase in the thermal conductivity with increasing temperature, in accordance with previously published data for undoped Mg_2Si.[40] The material with 1 vol% TiO_2 added shows a broader minimum in the thermal conductivity compared to the other materials and has the lowest value at 200 °C but the highest at 425 °C. For all materials the general trend of the thermal conductivity agrees with that of a semiconductor with increased conductivity at high temperatures where the intrinsic transition has occurred.

To evaluate if the increase in electrical conductivity of the materials with increasing titanium content could explain the limited effect of the nano-inclusions on the thermal conductivity, the electronic part of the thermal conductivity was calculated using the Wiedemann-Franz law $\kappa_{el} = L\sigma T$, with a Lorenz factor of 2.45×10^{-8} V^2 K^{-2} which is suitable for a semiconductor system.[40] The resulting values of the electronic part of the thermal conductivity of the prepared materials are presented in the inset of Fig. 4. As can be seen the values never exceed 0.25 W m^{-1} K^{-1} in the entire temperature range, and the difference between the materials is

no more than 0.05 W m^{-1} K^{-1}, implying that only a low fraction of the total thermal conductivity stems from the charge carriers. Thus the increased electrical conductivity cannot explain the limited effect of the nano-inclusions on the thermal conductivity of the materials. In some studies of Half Heusler compounds,[41,42] an increase in thermal conductivity has been reported upon introduction of nano-inclusions. The reasons for this were reaction of the nanoparticles, production of oxides with high thermal conductivity and the formation of complex phases. In our case it is possible that the relatively higher thermal conductivity, compared to the Mg_2Si matrix, of the included titanium containing compounds compensates for the expected increased grain boundary scattering achieved by the presence of these compounds. Another possibility is that the included compounds do not increase the concentration of grain boundaries enough in the material and therefore do not improve the scattering of phonons significantly and thus leave the thermal conductivity unchanged.

Thermoelectric figure-of-merit of prepared materials

The calculated ZT values of the prepared materials are presented in Fig. 5 as a function of temperature. The figure-of-merit shows a clear optimum when increasing the concentration of TiO_2 nanoparticles introduced into the Mg_2Si material during synthesis. The ZT values of the pure Mg_2Si material and the material with 3 vol% TiO_2 added are
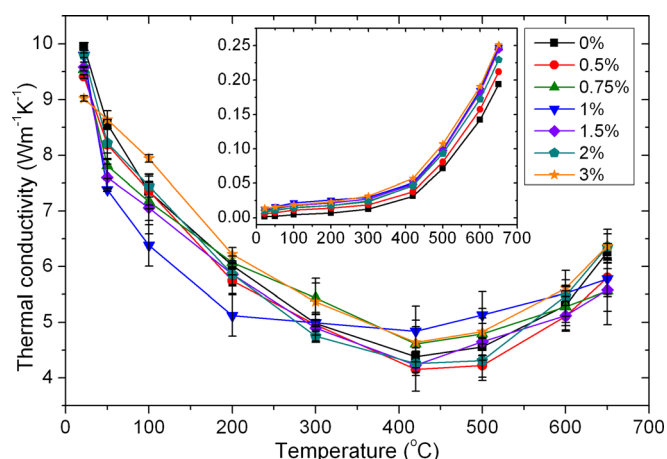
FIG. 4. (Color online) The thermal conductivity of Mg_2Si with the addition of 0–3 vol% TiO_2 nanoparticles as a function of temperature. The error bars show the standard deviation calculated from five measurements at each temperature. The inset shows the charge carrier part of the thermal conductivity calculated with the Wiedemann-Franz equation.
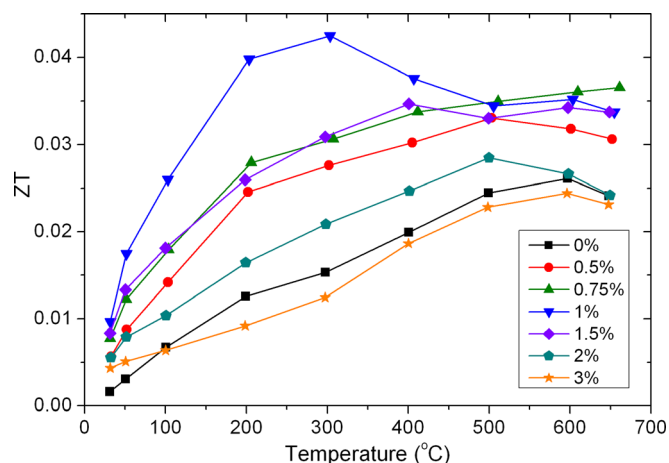
FIG. 5. (Color online) ZT values of Mg_2Si with the addition of 0–3 vol% TiO_2 nanoparticles, showing a clear ZT optimum for the sample to which 1 vol% TiO_2 was added.

very similar while the other materials show ZT values that are higher in the entire temperature range. The best performance is obtained with the material formed with 1 vol% TiO_2 added, which reaches its maximum in $ZT = 0.042$ at 300 °C. This is 2.75 times higher than the corresponding ZT value for the pure Mg_2Si material at the same temperature. The pure Mg_2Si sample reaches its maximum $ZT = 0.026$ at 600 °C, at which temperature the Mg_2Si material with 1 vol% TiO_2 added still shows a ZT value that is 1.35 times higher. As expected for Mg_2Si the ZT values for all materials are very low, but the increase in ZT with the TiO_2 addition represents a significant improvement. This is mainly achieved through the faster reduction in electrical resistivity compared to the Seebeck while the thermal conductivity was more or less unaffected by the introduction of titanium to the material. It is possible that a similar effect can be achieved even for more potent thermoelectric materials, such as the antimony-doped $Mg_2Si_xSn_{1-x}$. Especially if the thermal conductivity of the bulk material is already low, it would be interesting to explore if an improved optimum ratio between Seebeck coefficient and electrical resistivity as found here, can be reached by the addition of TiO_2 or other titanium-containing nanoinclusions.

CONCLUSIONS

The thermoelectric figure-of-merit of magnesium silicide-based materials was found to be improved by the addition of TiO_2 nanoparticles through mechanical and solvent free milling and subsequent spark plasma sintering of the mixtures. Within the concentration range of 0–3 vol% TiO_2 an optimal concentration was found at 1 vol% of added TiO_2, whereas the performance of Mg_2Si material with 3 vol% TiO_2 added showed similar ZT values as the pure Mg_2Si. The improvement in ZT for Mg_2Si with optimum addition of TiO_2 is achieved by a drastic reduction in electrical resistivity, which is accompanied by a less severe reduction in the absolute Seebeck coefficient. Thus the addition of 1 vol% TiO_2 nanoparticles to Mg_2Si resulted in the largest improvement of ZT at 300 °C, reaching $ZT = 0.042$ which is a factor 2.75 higher than the pure Mg_2Si at the same temperature. Upon sintering of the mixture of Mg_2Si and TiO_2 nanoparticles, the TiO_2 was completely reduced or reacted to $TiSi_2$ and possibly metallic titanium. Titanium atoms most likely enter the Mg_2Si matrix during the SPS process and donate electrons, explaining the observed increase in charge carrier concentration with a factor of 10, and the concurrent effects on the electrical conductivity and the Seebeck coefficient. Surprisingly, the thermal conductivity of the materials was not noteworthy affected by the introduction of TiO_2 nanoparticles, either due to that the higher thermal conductivity of the titanium containing compound, compared to Mg_2Si, present in the materials compensates for the increased number of grain boundaries scattering the phonons and the charge carriers, or due to too few introduced additional grain boundaries to achieve the expected behavior. Even though the ZT values of the prepared materials remain low, as expected for pure Mg_2Si, the increase achieved by the introduction of TiO_2 nanoparticles is significant and this

system may serve as a model for improving the properties of the more prominent thermoelectric system $Mg_2Si_{1-x}Sn_x$.

[1]B. C. Sales, Science **295**, 1248 (2002).
[2]G. J. Snyder, Electrochem. Soc. Interface **17**, 54 (2008).
[3]C. T. Hsu, D. J. Yao, K. J. Ye, and B. Yu, J. Renew. Sustain. Energy **2**, 013105 (2010).
[4]G. A. Slack, in *CRC Handbook of Thermoelectrics*, edited by D. M. Rowe (CRC Press LLC, Boca Raton, 1995).
[5]G. J. Snyder and E. S. Toberer, Nature Mater. **7**, 105 (2008).
[6]M. S. Dresselhaus, G. Dresselhaus, X. Sun, Z. Zhang, S. B. Cronin, T. Koga, J. Y. Ying, and G. Chen, Microscale Thermophys. Eng. **3**, 89 (1999).
[7]L. D. Hicks and M. S. Dresselhaus, Phys. Rev. B **47**, 16631 (1993).
[8]L. D. Hicks, T. C. Harman, and M. S. Dresselhaus, Appl. Phys. Lett. **63**, 3230 (1993).
[9]L. D. Hicks, T. C. Harman, X. Sun, and M. S. Dresselhaus, Phys. Rev. B **53**, R10493 (1996).
[10]J. P. Heremans, C. M. Thrush, D. T. Morelli, and M.-C. Wu, Phys. Rev. Lett. **88**, 216801 (2002).
[11]J. L. Mi, X. B. Zhao, T. J. Zhu, and J. P. Tu, Appl. Phys. Lett. **91**, 172116 (2007).
[12]Z. Xiong, X. Chen, X. Huang, S. Bai, and L. Chen, Acta Mater. **58**, 3995 (2010).
[13]T. C. Harman, P. J. Taylor, M. P. Walsh, and B. E. LaForge, Science **297**, 2229 (2002).
[14]J. C. Caylor, K. Coonley, J. Stuart, T. Colpitts, and R. Venkatasubramanian, Appl. Phys. Lett. **87**, 023105 (2005).
[15]T. Harman, M. Walsh, B. Laforge, and G. Turner, J. Electron. Mater. **34**, L19 (2005).
[16]A. J. Minnich, M. S. Dresselhaus, Z. F. Ren, and G. Chen, Energy Environ. Sci. **2**, 466 (2009).
[17]M. Zebarjadi, Z. Bian, R. Singh, A. Shakouri, R. Wortman, V. Rawat, and T. Sands, J. Electron. Mater. **38**, 960 (2009).
[18]M. Zebarjadi, K. Esfarjani, A. Shakouri, J.-H. Bahk, Z. Bian, G. Zeng, J. Bowers, H. Lu, J. Zide, and A. Gossard, Appl. Phys. Lett. **94**, 202105 (2009).
[19]W. Kim, J. Zide, A. Gossard, D. Klenov, S. Stemmer, A. Shakouri, and A. Majumdar, Phys. Rev. Lett. **96**, 045901 (2006).
[20]L. D. Chen, X. Y. Huang, M. Zhou, X. Shi, and W. B. Zhang, J. Appl. Phys. **99**, 064305 (2006).
[21]Z. M. He, C. Stiewe, D. Platzek, G. Karpinski, E. Muller, S. H. Li, M. Toprak, and M. Muhammed, J. Appl. Phys. **101**, 043707 (2007).
[22]J. L. Mi, X. B. Zhao, T. J. Zhu, and J. P. Tu, J. Phys. D: Appl. Phys. **41**, 205403 (2008).
[23]Ø. Prytz, A. E. Gunnæs, O. B. Karlsen, T. H. Breivik, E. S. Toberer, G. Jeffrey Snyder, and J. Taftø, Philos. Mag. Lett. **89**, 362 (2009).
[24]D. L. Medlin and G. J. Snyder, Curr. Opin. Colloid Interface Sci. **14**, 226 (2009).
[25]S. V. Faleev and F. Leonard, Phys. Rev. B **77**, 9 (2008).
[26]J. M. O. Zide, J. H. Bahk, R. Singh, M. Zebarjadi, G. Zeng, H. Lu, J. P. Feser, D. Xu, S. L. Singer, Z. X. Bian, A. Majumdar, J. E. Bowers, A. Shakouri, and A. C. Gossard, J. Appl. Phys. **108**, 123702 (2010).
[27]V. K. Zaitsev, M. I. Fedorov, E. A. Gurieva, I. S. Eremin, P. P. Konstantinov, A. Y. Samunin, and M. V. Vedernikov, in Proceedings of the 24th International Conference on Thermoelectrics (IEEE, New York, 2005), pp. 204-210.
[28]T. Aizawa and R. Song, Intermetallics **14**, 382 (2006).
[29]J. I. Tani and H. Kido, Jpn. J. Appl. Phys., Part 1 **46**, 3309 (2007).
[30]J. I. Tani and H. Kido, Physica B **364**, 218 (2005).

[31] Z. Xiong, X. H. Chen, X. Y. Zhao, S. Q. Bai, X. Y. Huang, and L. D. Chen, Solid State Sci. **11**, 1612 (2009).

[32] D. Cederkrantz, M. Nygren, and A. E. C. Palmqvist, J. Appl. Phys. **108**, 113711 (2010).

[33] S. E. Gustafsson, Rev. Sci. Instrum. **62**, 797 (1991).

[34] K. Kondoh, H. Oginuma, E. Yuasa, and T. Aizawa, Mater. Trans. **42**, 1293 (2001).

[35] M. Yoshinaga, T. Iida, M. Noda, T. Endo, and Y. Takanashi, Thin Solid Films **461**, 86 (2004).

[36] J. F. Jongste, O. B. Loopstra, G. C. A. M. Janssen, and S. Radelaar, J. Appl. Phys. **73**, 2816 (1993).

[37] A. L. Patterson, Phys. Rev. **56**, 978 (1939).

[38] H. J. Goldsmid and J. W. Sharp, J. Electron. Mater. **28**, 869 (1999).

[39] M. W. Heller and G. C. Danielson, J. Phys. Chem. Solids **23**, 601 (1962).

[40] M. Akasaka, T. Iida, A. Matsumoto, K. Yamanaka, Y. Takanashi, T. Imai, and N. Hamada, J. Appl. Phys. **104**, 013703 (2008).

[41] R. Yaqub, P. Sahoo, J. P. A. Makongo, W. M. Nolting, N. Takas, P. F. P. Poudeu, and K. L. Stokes, in *Thermoelectric Materials - Growth, Properties, Novel Characterization Methods, and Applications*, edited by H. L. Tuller, J. D. Baniecki, G. J. Snyder, and J. A. Malen (Mater. Res. Soc. Symp. Proc., Warrendale, PA, 2010), Vol. 1267, p. DD05-18.

[42] J. P. A. Makongo, P. Paudel, D. K. Misra, and P. F. P. Poudeu, in *Thermoelectric Materials - Growth, Properties, Novel Characterization Methods, and Applications*, edited by H. L. Tuller, J. D. Baniecki, G. J. Snyder, and J. A. Malen (Mater. Res. Soc. Symp. Proc., Warrendale, PA, 2010), Vol. 1267, p. DD07-10.